Developing Fuel Efficiency and CO_2 Emission Maps of a Vehicle Engine Based on the On-Board Diagnostic (OBD) Approach

Fredy Rosero[1], Xavier Rosero[2], Zamir Mera[3]

***Abstract* — In real traffic conditions vehicle interacts with the road, other vehicles, and traffic control devices. The level of traffic influences driving patterns and, consequently, this can affect the vehicle's fuel efficiency and emissions. This study aims to develop engine maps of fuel consumption and carbon dioxide (CO_2) emissions for a light vehicle operating under real traffic conditions. A representative passenger vehicle powered by gasoline of the ecuadorian vehicle fleet was selected for the experimental campaign that was developed on a test route designed according to real driving emission (RDE) regulation. An on-board diagnostic (OBD) device was used for recording in real-time engine and vehicle operating parameters. Moreover, CO_2 emissions were estimated using the fuel rate registered from the OBD system of the vehicle This study proposed a novel methodology for developing two-dimensional contour engine maps based on OBD data. The result showed that the vehicle engine operated in real traffic conditions with a brake thermal efficiency (BTE) of 27 %, a brake-specific fuel consumption (BSFC) of 275 g/kWh, and a CO_2 energy-emission factor of 716 g/kWh. In terms of distance, the CO_2 emission factor for the tested vehicle was approximately 190 g/km. Overall, this study demonstrates that the OBD approach is a potential method to be used to assess the fuel consumption and CO_2 emissions of a vehicle operating under real-world traffic conditions, especially in Latin American countries, where portable emission measurement systems (PEMS) are not readily available.**

***Keywords* — Fuel Consumption; *CO2* Emissions; Engine Maps; On-Board Diagnostic (OBD).**

***Resumen* — En condiciones reales de circulación un vehículo interactúa con la carretera, con otros vehículos y con los dispositivos de control del tráfico. El nivel de tráfico influye en los patrones de conducción y, en consecuencia, esto puede afectar a la eficiencia del combustible y las emisiones del vehículo. El objetivo de este estudio es desarrollar mapas motorizados de consumo de combustible y emisiones de dióxido de carbono (CO_2) para un vehículo ligero que circule en condiciones reales de tráfico. Un vehículo de pasajeros propulsado a gasolina y representativo del parque automotor ecuatoriano fue seleccionado para la campaña experimental que se desarrolló en una ruta de prueba diseñada de acuerdo a la normativa de emisiones en conducción real (RDE). Se utilizó un dispositivo de diagnóstico a bordo (DAB) para registrar en tiempo real los parámetros de funcionamiento del motor y del vehículo. Además, las emisiones de CO_2 se estimaron utilizando la tasa de combustible registrada desde el sistema OBD del vehículo. Este estudio propuso una metodología novedosa para desarrollar mapas de motor de contorno bidimensional basados en datos OBD.**

El resultado mostró que el motor del vehículo funcionaba en condiciones reales de tráfico con una eficiencia térmica de frenado (ETF) del 27 %, un consumo de combustible específico de frenado (CCFE) de 275 g/kWh y un factor de emisión de energía de CO_2 de 716 g/kWh. En términos de distancia, el factor de emisión de CO_2 del vehículo probado fue de aproximadamente 190 g/km. En general, este estudio demuestra que el enfoque OBD es un método potencial para ser utilizado para evaluar el consumo de combustible y las emisiones de CO2 de un vehículo que opera en condiciones de tráfico del mundo real, especialmente en los países de América Latina, países en los que los sistemas portátiles de medición de emisiones (PEMS) no están fácilmente disponibles.

***Palabras clave* — Consumo de combustible; Emisiones de CO_2; Mapas de motor; Diagnóstico a bordo (OBD).**

I. INTRODUCTION

In cities around the world, road transport is a major source of greenhouse gas (GHG) emissions and air pollution, affecting the environment and human health, respectively. From 2022 to 2050, global energy consumption for road transport is projected to increase by 28 % [1]. In Ecuador, the energy balance calculated for 2021 by the Ministry of Energy and Mines estimates that transport with approximately 49 % is the sector that showed the highest energy consumption. In fact, diesel and gasoline were the energy sources with the highest demand, with annual growth rates of up to 25 % [2]. As a result, the sector with the highest GHG emissions in Ecuador in 2021 was transport with 50.7 %. Hence, the energy and environmental problems produced by road transport cannot be ignored.

Fuel consumption and emissions of vehicles under real traffic conditions are the result of the interaction of several factors and conditions [3]. In general, these conditions can be categorized into: (I) vehicle design (for example, vehicle type, powertrain configuration and technology, fuel type and aftertreatment system technology). (II) driver characteristics. (III) travel conditions (for example, passenger load and use of auxiliary systems). (IV) traffic flow conditions (for example, congestion). (V) road conditions (for example, slope level and road type). (VI) environmental conditions (for example, temperatu-

[1] Corresponfing author: Fredy Rosero Ph.D. of the Faculty of Applied Sciences, Universidad Técnica del Norte, 100105 Ibarra, Ecuador (e-mail: farosero@utn.edu.ec). ORCID number 0000-0003-0971-1944.

[2] Xavier Rosero Ph.D. of the Faculty of Applied Sciences, Universidad Técnica del Norte, 100105 Ibarra, Ecuador (e-mail: cxrosero@utn.edu.ec). ORCID number 0000-0002-5396-6621.

[3] Zamir Mera Ph.D. of the Faculty of Applied Sciences, Universidad Técnica del Norte, 100105 Ibarra, Ecuador (e-mail: zamera@utn.edu.ec). ORCID number 0000-0003-2897-8847.

Manuscript Received: Sep 21, 2023
Revised: Nov 08, 2023
Accepted: Nov 27, 2023
DOI: https://doi.org/10.29019/enfoqueute.1002

re). And (VII) geographical conditions (for example, altitude). Hence, unlike laboratory testing with controlled conditions, evaluation under real traffic conditions is a strategy that the scientific community is currently applying to obtain real-world vehicle performance.

In recent times, several studies have reported that vehicles show significant differences between the emission levels measured experimentally in real traffic conditions and the levels obtained in vehicle type-approval processes with controlled operating conditions. This has led to additional and rapid changes in enforcement in the United States [4], China and the European Union [5]. In fact, Europe already requires the use of portable emission measurement systems (PEMS) and on-board diagnostic (OBD) systems to verify vehicle emissions, both for type-approval and real-traffic testing [6]. In Latin America, Brazil has adopted OBD requirements like the Euro V standard. In the case of OBD systems, they have been designed to monitor the performance of the engine and aftertreatment system components of the vehicles. Consequently, OBD systems have become a key component of vehicle inspection and maintenance programs, as well as for verifying that a vehicle meets regulatory compliance limits [7]. In general, PEMS measurements and OBD data collection are the two strategies commonly applied worldwide to assess the performance of vehicles and engines in real-traffic conditions. However, in Latin America PEMS equipment is not widely available. Hence, the OBD approach becomes a valid strategy to be applied in studies developed in countries such as Ecuador.

In parallel, to minimize discrepancies between type-approval emission levels and those in real traffic, the European Union has introduced the Regulation (EU) 2016/427 [8], which includes a testing procedure called 'Real Driving Emissions' (RDE) as a complement to the globally harmonized light-duty vehicle test cycles (WLTC) [9]. RDE test method is based on the use of PEMS to monitor on-road emission levels of light-duty vehicles. In addition, the routes defined in the RDE tests need to meet certain characteristics: environmental, dynamic, driving behaviour and equipment accuracy, among others described in the Regulation (EU) 2017/115 [10]. Therefore, the design of a test route according to the RDE regulation would be a strategy to improve the reliability of the data obtained in a study.

Previous work has focused on assessing the fuel efficiency and emission levels of vehicles using four approaches: (a) emission modelling and vehicle simulators, (b) vehicle specific power (VSP) based assessments, (c) real traffic testing with PEMS, and (d) engine map development. Some relevant work for each approach can be mentioned below. In the case of emission modelling, Wen et al. [11] recently used a random forest model to map real-time vehicle emissions on a motorway in Chengdu (China). Regarding the VSP approach, this was used by He et al. [12] to develop and statistically compare VSP distributions as a function of speed and vehicle typology in Beijing. In the case of experimental PEMS data, Bishop et al. [13] used it to identify discrepancies in fuel efficiency and nitrogen oxide (NO_x) emissions between homologation processes and real traffic for various diesel and gasoline vehicle models. Regarding engine maps, Mera et al. [14] combined engine operation data and the VSP approach to reduce emission estimation error. It can also be mentioned that Castresana et al. [15] recently investigated the robustness of artificial neural networks to predict multiple performance and emission parameters using information from a diesel engine map for marine applications. In general, the engine mapping approach characterizes the fuel consumption and emission performance of a vehicle's engine for different engine speed and torque ranges [16]. In addition, this resulting information is very useful as input data for emission models and vehicle simulators.

Based on the literature review, three gaps were identified concerning engine maps: (I) maps have not been developed using only data from the vehicle's OBD system. (II) transient maps have not been constructed from a vehicle operating under a test route designed according to RDE regulations. (III) in Latin America, the engine map approach has not been applied to assess vehicle performance. Hence, this study focuses on the development of engine maps of fuel consumption and carbon dioxide (CO_2) emissions for a vehicle operating under real traffic conditions on an RDE test route in the city of Ibarra, Ecuador.

There are three research questions posed for this study:

- Is it possible to develop contour engine maps using information from the OBD system of a light-duty vehicle operating in real traffic?
- What are the most used torque and RPM ranges in engine maps of a vehicle operating on an RDE test route?
- How do fuel efficiency and CO_2 emission levels vary for different engine map zones?
- What are the average fuel consumption and CO_2 emission factors of a light-duty vehicle for the motorway, suburban and urban sections of the RDE route?

II. METHODOLOGY

A. Test vehicle

A representative passenger vehicle powered by gasoline of the ecuadorian vehicle fleet was selected to analyze the performance of an engine in real traffic conditions. In fact, in the last decade, this vehicle has been one of the most used models for the taxi service in several cities of Ecuador [17]. The tested vehicle was a Chevrolet Aveo Emotion, equipped with an engine of 1.6 liters. In general, the characteristics of the test vehicle are representative of passenger capacity, weight, engine torque and power and gearbox type for the automotive segment of the country. Table I provides additional information of the tested vehicle. Moreover, it is important to note that the tested vehicle underwent an exhaustive preventive and corrective maintenance program to guarantee the results of this study. In fact, this maintenance ensured that the vehicle successfully passed the mandatory annual technical inspection required by ecuadorian regulations. Consequently, the evaluated vehicle was in optimal technical condition before the execution of the experimental campaign.

TABLE I
TECHNICAL SPECIFICATIONS OF THE TESTED VEHICLE

Vehicle parameter	Value
Fuel type	Gasoline
Model name	Chevrolet Aveo Emotion
Model year	2011
Gross vehicle weight (t)	1.592
Weight (t)	1.203
Length /Width/ Height (m)	4.04/1.67/1.16
Max passengers	5
Axle configuration	4×2
Gearbox	Manual (5)
Number of engine cylinders	4 in-line
Engine total displacement (cm^3)	1598
Engine maximum power (kW@rev/min)	76@5800
Engine peak torque (N.m@rev/min)	145@3600
Fuel injection type	Indirect injection
Compression ratio	9.5:1

B. Test route

In this study, an experimental campaign was conducted along a test route designed in the city of Ibarra, Ecuador. This city is the capital of the province of Imbabura and has a population of approximately 200 000 inhabitants. In terms of vehicle fleet, Ibarra has experienced a significant growth of approximately 6 % per year in recent years [18], which has generated challenges in terms of traffic and mobility. In this study, the test route was designed under the regulation (EU) 2017/1151 [10], which establishes different kinematic parameters, such as distance by route section, vehicle speeds, cumulative altitudes, and total trip duration. Hence, this study was carried out on an RDE test route (with approximately 53 km) including urban (0-60 km/h), suburban (60-90 km/h), and motorway (>90 km/h) sections, as shown in Fig. 1. However, it is important to mention that this study is not intended to represent an RDE homologation process to evaluate the fuel consumption and CO_2 emissions of the vehicle. In addition, details of the test route are provided in Table II.

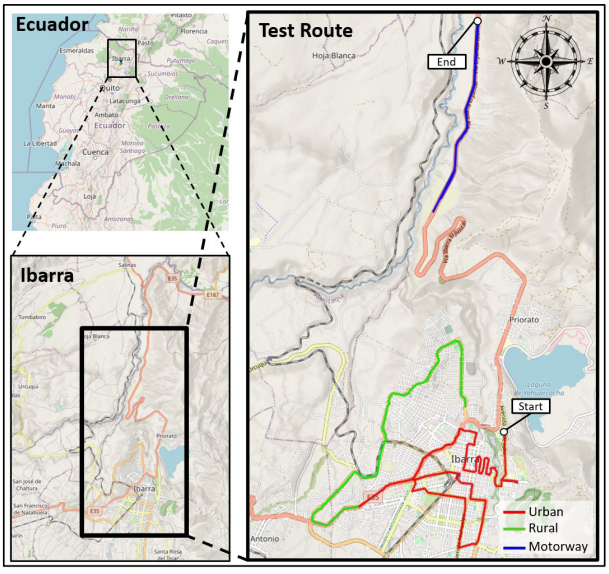

Fig. 1. Selected experimental route for field data collection.

TABLE II
INFORMATION OF TEST ROUTE

Start position	Avenue 17 de Julio
Final position	Panamericana Norte E-35
Altitude at origin/destination position (m)	2219/1853
Total trip distance (km)	52.8
Urban trip distance (km)	19.1
Suburban trip distance (km)	12.3
Motorway trip distance(km)	21.4
Altitude difference (m)	366

C. Instrumentation

In general, the study required instruments for measuring the following three types of information: (I) vehicle kinematics (for example, position and speed), (II) vehicle and engine operating parameters (for example, torque and speed engine values), and (III) instantaneous fuel consumption data. A global positioning system (GPS) logger device, called 'GL-770', was installed in the test vehicle to record latitude, longitude, altitude, and vehicle speed with a frequency of 1Hz. It is important to note that this device is non-intrusive, resulting in the collection of vehicle kinematic information without affecting the regular operation of the tested vehicle operation. To record engine operating parameters and the vehicle fuel consumption data, an OBD interface device (called ELM Electronics 327) was connected to a mobile phone application (called Torque Pro). The ELM 327 was connected to the OBD2 diagnostic port to read the engine operating parameters in real time from the engine control unit (ECU). At the same time, these parameters were sent via Bluetooth from the ELM 327 to the Torque Pro mobile application to be recorded. In this study, the paid version of Torque Pro was used to set the 1 Hz sampling time of the data. The three instruments used for field data collection are shown in figure 2.

Fig. 2. Tested vehicle equipped on board with GPS logger, OBD interface, and OBD data recording application for field data collection.

D. Experimental campaign

As mentioned above, a Chevrolet Aveo vehicle equipped with GPS and OBD interface devices was evaluated on a test route in the city of Ibarra. The experimental campaign of this study was conducted in February 2023. The campaign for the tested vehicle included both peak (7:00 and 13:00) and non-peak (10:00 and 15:00) periods. The vehicle was driven normally on the test route, respecting the traffic signals and speed limits established in the city. During the experimental campaign, the vehicle was powered by a commercially available type of gasoline called 'Extra' in Ecuador. This gasoline is characterised by an octane number of 85. The air conditioning of the vehicle was turned off to avoid additional loads on the engine operation during the experimental campaign. Before the start of each test, the vehicle was warmed up for 15 minutes until the engine reached normal operating temperature. To ensure the repeatability of the tests, the same driver drove the vehicle during all tests. Regarding the passenger load, the campaign was conducted with two people: a driver and a staff technician. The experimental campaign included six entire trips on the RDE route. These tests were conducted during peak periods (7:00 and 13:00) and off-peak periods (10:00 and 15:00). This strategy was designed to ensure that the results obtained accurately reflected vehicle performance at different levels of congestion. The average duration of each entire trip (urban, suburban and motorway road sections) on the test route was approximately 1.7 hours, and the average trip speed of the vehicle was approximately 35 km/h. Table III shows an overview of the operating conditions for the tested vehicle by road section in the experimental campaign.

TABLE III
OVERVIEW OF THE OPERATING CONDITIONS FOR THE TESTED VEHICLE IN TERMS OF THE ROAD SECTION IN THE EXPERIMENTAL CAMPAIGN

Operating condition	Road section			All sections
	Urban	Suburban	Motorway	
Tests	6	6	6	6
Average trip time (s)	5 040	820	846	6 084
Average trip speed (km/h)	18.35	53.39	92.77	35.01
Average moving speed (km/h)	25.42	58.35	93.73	44.24
Maximum trip speed (km/h)	55.64	85.52	115.16	115.16
Average positive accel (m/s^2)	0.45	0.44	0.28	0.41
Total idle period (%)	28.06	8.49	1.01	21.04
Total accel period (%)	32.4	39.51	31.33	33.24
Total decele period (%)	27.29	33.85	29.93	28.63
Total cruise period (%)	12.24	18.13	37.7	17.08

E. Pre-processing real-world vehicle data

In this study, the applied preprocessing method was developed using R Studio software [19]. As the measurements of the experimental campaign were recorded using two devices with different initial recording times, a preprocessing step was developed to synchronise the different signals from the two devices through the vehicle speed. This speed was recorded second-by-second using both the GPS position data and through the OBD system of the vehicle. It is important to mention that the speed profiles were smoothed using a moving window filter [20]. Overall, the data pre-processing stage ensures to guarantee of the results presented in this study.

F. Method for developing engine maps based on OBD data

Three variables are necessary in order to develop an engine map graph. Typically, torque and speed are used as the primary factors for the horizontal and vertical axes of the maps. Meanwhile, the third variable (Brake Thermal Efficiency (BTE), fuel consumption, brake-specific fuel consumption (BSFC) and emission rates) served as the parameter defining the theme of the map. In this study, the method applied to develop the engine maps included the following two stages: (1) generate grid engine maps by engine speed and torque ranges with averaged values of the third variable, and (2) develop two-dimensional contour engine maps based on grid data. These two stages were performed using R Studio [19].

Initially, the grid engine maps were developed following the methodology proposed by Rosero et al. [21]. Initially, grids were generated based on torque and speed engine intervals, and the remaining engine operating data (referred to as the third variable) were assigned to their corresponding grid. Subsequently, the grouped data were averaged to obtain a single value by grid (speed-torque). Outliers were filtered by examining the relative frequency and standard deviation of each data group. Finally, the averaged values were discretized and assigned specific colours for each data interval when plotted on the engine maps.

Subsequently, to plot the two-dimensional contour engine maps, this study utilized the RStudio software [19] with an R package called 'ggplot2' R [22]. This package includes a function named 'geom_contour_filled()', which generates contour plots using z variable observations (for example, fuel consumption, and emission rates) that should be previously grouped into interval combinations of two variables, x (engine speed) and y (torque). Based on this requirement, the data matrices resulting from the grid engine were used as input data to generate the contour engine maps. Finally, to develop the Contour-plot engine maps, a divergent colour scale was applied for each defined interval of the third variable. As a result of these two processing stages, this study obtained contour maps of BTE, BSFC, brake-specific CO_2 emissions, fuel consumption rates and CO_2 rates.

III. CALCULATION METHODS

A. Effective power and torque of the engine

The OBD system provided engine load values $(L_{e_{obd}})$ as a percentage relative to the maximum effective power $(P_{e_{max}})$that the engine could produce. Based on the technical specifications of the tested vehicle manufacturer, the $P_{e_{max}}$ assumed for this study was 76 kW. To determine the actual effective engine power (P_e) in kW at any given moment, equation 1 was utilized.

Equation 1

$$P_e = L_{e_{obd}} \cdot P_{e_{max}} \quad (1)$$

The instantaneous engine torque values (τ) expressed in N.m, were calculated by multiplying the effective power and the engine speed.

B. Fuel energy efficiency and CO_2 emission factors

The grid engine map generation process involved the calculation of the second-by-second BTE and BSFC values expressed in $(\%)$ and (g/kWh), respectively, for the tested engine. These calculations were performed using equation 2 and 3, as follows:

Equation 2

$$BTE = \frac{P_e}{P_{th}} = \frac{P_e}{FC \cdot CV_{fuel}} \quad (2)$$

Equation 3

$$BSFC = \frac{3600 \cdot FC}{P_{-}} \quad (3)$$

Here, FC is the instantaneous fuel consumption expressed in (g/s), P_{th} represents the instantaneous thermal power (kW) resulting from the fuel being injected, while CV_{fuel} is the calorific value of the gasoline used $(46.3\ MJ/kg)$ [23].

In this study, based on the stoichiometry of gasoline combustion, the CO_2 emission rate (ER_{CO_2}) was calculated using equation 4 as follows:

Equation 4

$$ER_{CO_2} = FC \cdot \frac{44}{12+\left(\frac{H}{C}\right)} \quad (4)$$

Here, since the fuel utilized is gasoline (C_8H1_8), the assumed values were 18 for hydrogen (H) and 8 for carbon (C) [24].

To assess the performances of the tested engine for different road sections (i), the average values of BTE (%), BSFC (g/kWh), energy-specific CO_2 emission factor (g/kWh), as well as fuel consumption and CO_2 emission rates (g/s), were estimated using equations 5-9, as follows:

Equation 5

$$\overline{BTE_i} = \frac{\sum_{t=1}^{T_i}(BTE_i)}{T_i} \quad (5)$$

Equation 6

$$\overline{BSFC_i} = \frac{\sum_{t=1}^{T_i}(BSFC_i)}{T_i} \quad (6)$$

Equation 7

$$\overline{EF_{CO_2\,i}}^{e} = \frac{\sum_{t=1}^{T_{i,w}}\left(EF_{CO_{2\,i,}}\right)}{T_i} \quad (7)$$

Equation 8

$$\overline{FC_i} = \frac{\sum_{t=1}^{T_i}(FC_i)}{T_i} \quad (8)$$

Equation 9

$$\overline{ER_{CO_2\,i}} = \frac{\sum_{t=1}^{T_{i,w}}\left(ER_{CO_{2\,i,}}\right)}{T_i} \quad (9)$$

Here, T is the number of second-by-second test data.

Moreover, to evaluate the vehicle performance for different road sections, the average distance-specific fuel consumption $(\overline{FC}^d)$ and CO_2 emission $(\overline{EF_{CO_2}}^d)$ factors, expressed in (g/km), were estimated using equations 10 and 11, as follows:

Equation 10

$$\overline{FC_i}^d = \frac{\sum_{t=1}^{T_i}(FC_{i,t})}{\sum_{t=1}^{T_i}(d_t)} \quad (10)$$

Equation 11

$$\overline{EF_{CO_2\,i}}^d = \frac{\sum_{t=1}^{T_i}\left(ER_{CO_{2\,i,t}}\right)}{\sum_{t=1}^{T_i}(d_t)} \quad (11)$$

IV. RESULTS AND DISCUSSION

The results provided in this section address the research questions and are organized into three topics: (a) typical engine operation patterns by torque and speed for different road sections, (b) contour engine maps of BTE, fuel efficiency, and CO_2 emissions, and (c) the overall fuel consumption and emission factors.

A. Typical engine operation patterns by torque and speed

Figure 3 presents the patterns of engine operation by torque and speed for motorway, suburban, and urban roads. Grey circles represent the cumulative relative frequency (CRF) of engine operation points calculated for each torque and speed interval, while yellow shaded areas identify the highest engine operation patterns. In the case of the motorway section, the engine operated approximately 85 % of the time in a speed range of 2 500-3 500 rev/min, which are half-load intervals considering that the maximum engine power is reached at 5 800 rev/min. On the suburban section, engine performance was heterogeneous, operating approximately 95 % between low and high (75–100 N·m) torque ranges and low and medium (3 000-3 500 rev/min) speed ranges. In the case of the urban section, approximately 50 % of engine operation was between the lowest torque and lowest speed ranges. Based on Table II, these low-load operation results for urban roads are related to the fact that the vehicle operated with approximately 30 % at idle conditions and an average travel speed of less than 20 km/h. Overall, these results demonstrate that the type of road section significantly influences the torque and speed

ranges that a vehicle engine can operate in real traffic conditions. This is consistent with that reported by Bishop et al. [25], who also found that the engine load patterns can vary with the type of road section, especially due to large changes in vehicle kinematics. In fact, Bishop et al. found that a light passenger vehicle engine ran approximately 35 % in low (90-110 N·m) torque ranges and low (1 000-1 500 rev/min) speed ranges. This value of 35 % operation at low load conditions is slightly higher than the 30 % found in the present study. Moreover, Tsiakmakis et al. [26] reported that the average travel speed and $v*a$ factors for light passenger vehicles (LDVs) vary significantly with the type of road section. In fact, Tsiakmakis et al. found that between motorway and urban sections, the average trip speed was reduced approximately 3.5 times (from 67 to 19 km/h). Whereas, in the present study, this speed was strongly reduced by 5 times (from 92 to 18 km/h).

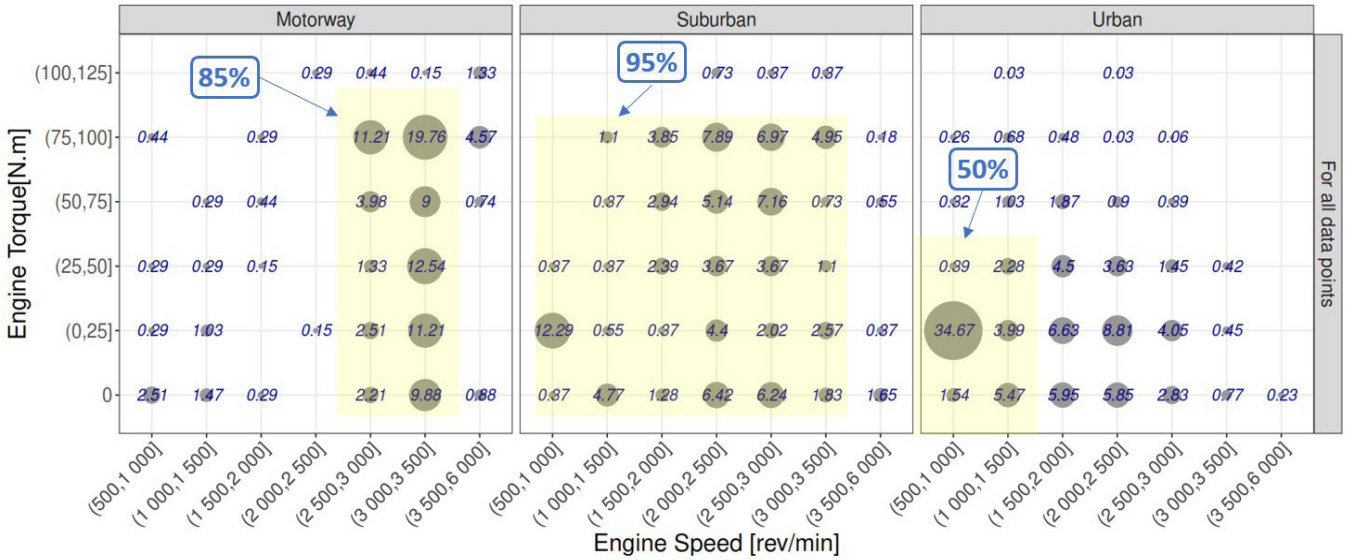

Fig. 3. Typical engine operation patterns by type of road section for all data points

B. Contour engine maps based on OBD data

1. Fuel energy efficiency and brake-specific CO_2 emission maps

Figure 4 illustrates the contour engine maps for BTE (a), BSFC (b), and brake-specific CO_2 emissions (c). In figure 4. a) the areas with the highest BTE (light green) values correspond to operating ranges with medium torque and engine speed, while those with the lowest efficiency (blue) are in areas of low torque demand. Additionally, at high torque and speed ranges, the engine shows values above 25 %. In figure 4.b) and 4.c) it can be seen that the contours with the lowest fuel efficiency and brake-specific CO_2 emissions (respectively) are in low torque ranges, which are common for an engine running in idle mode. Figure 4. b) shows that the largest contour corresponds to a range of BSFC with values between 175 and 250 g/kWh. This range is typical for engines mounted on light vehicles [27]. Figure 4.c) shows that the lowest CO_2 emissions (light green) areas with values below 600 g CO_2/kWh are in the mid-range of torque and speeds. Overall, these results indicate that the lowest fuel consumption and CO_2 emissions correspond to medium torque and engine speed ranges. Similar patterns were found by previous studies that evaluated engine performance of engines based on the engine mapping approach [13], [25]. In fact, Bishop et al. [13] found that between medium and high load conditions, the brake-specific CO_2 emissions of an engine were reduced by approximately 2.5 times (from 500 to 200 g CO_2/kWh). Moreover, these three figures show that in idle mode, which is typical of urban operation conditions, the engine has a lower fuel efficiency in terms of energy.

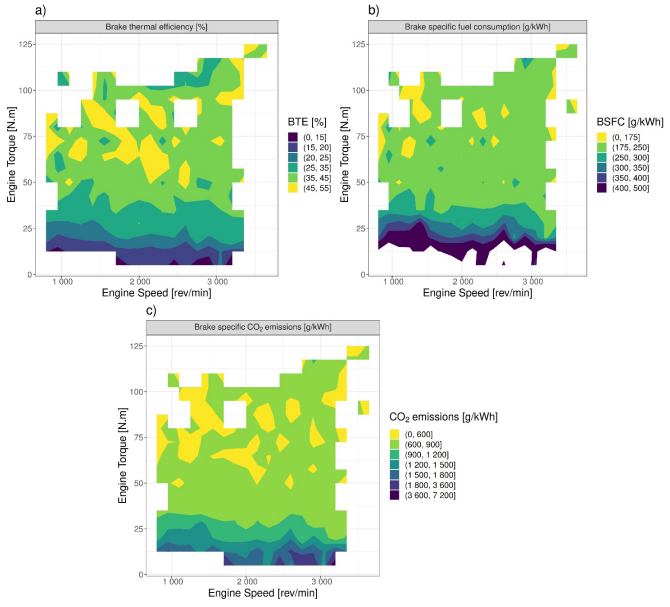

Fig. 4. Engine maps for (a) brake thermal efficiency, (b) brake-specific fuel consumption, and (c) brake-specific CO_2 emissions.

2. Fuel consumption and emission rates maps

Figure 5.a) and 5.b) present contour engine maps for fuel consumption and CO_2 emissions rates, respectively. Overall, these figures have similar sharply increasing trends (from light green to blue areas) of strong increase. In fact, Figure 5.a) and 5.b) show that the engine under maximum power operating conditions with an increase in torque and speed, fuel consumption and CO_2 emissions rates reached the highest values (blue) of 3.5 and 10.0 g/s, respectively. In contrast, as expected, when there is a lower demand for engine power, the fuel consumption and emission rates have the lowest values (light green). Although these green areas show lower fuel consumption expressed in terms of rates, based on Figure 6, it can be stated that these same areas are the least efficient in energy terms. The resultant increasing trends are consistent with previous works for LDV's [13], [14], [28] and heavy-duty vehicles (HDV's) [21], [29], and emissions models [30]. For instance, Mera et al. [13] found that between low and high load conditions, the CO_2 emissions rates of an LDV engine increased approximately 20 times (from 0.32 to 7.2 g CO_2/s). Similarly, in the present study, the CO_2 emissions rates were increased by about 14 times (from 0.69 to 10 g CO_2/s). It is important to note that the information contained in figure 5, expressed in terms of (g/s), can be used as input data to develop an empirical emission model. Previously, the information from the maps must be arranged in the form of a matrix by torque and engine speed intervals [21], [31]. The model can predict second-by-second fuel consumption and CO_2 emission values of the vehicle for any given operating scenario. Hence, future work will focus on using the engine map matrix resulting from this study for predicting fuel consumption and emissions of a vehicle by using torque and speed signals from engine operation as input data.

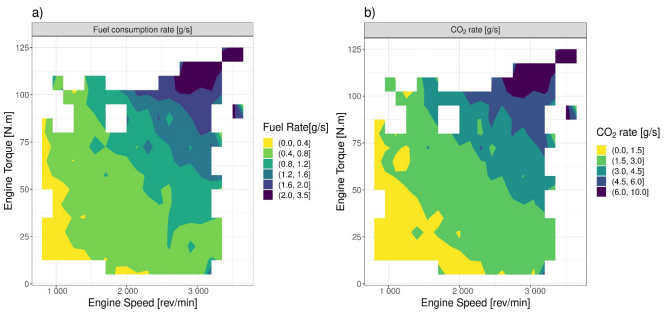

Fig. 5. Engine maps for (a) fuel consumption, and (c) CO_2 rates.

C. Overview of vehicle engine performance

Table IV shows the overall engine performance of the tested vehicle for motorway, suburban, and urban road sections. The performance of the vehicle is expressed in terms of energy-emission factors, average emission rates and distance-emission factors. In the case of BTE, the average value was 27 % for all sections, although in urban a BTE of approximately 25 % was found. This result is consistent with figure 3 and 4, which showed that in urban conditions, the engine frequently ran in low torque and speed ranges, where there was lower fuel efficiency. In the case of energy-emission factors, this study found an average value of BSFC and CO_2 of approximately 275 and 716 g/kWh, respectively. The minimum BSFC was for the motorway section with 250.18 g/kWh. In the case of the CO_2 emission factor in terms of distance, the average value was approximately 190 g/km. Comparing urban and motorway road sections, CO_2 emission factors of the vehicle increase by up to 50 %. The average value of 190 g CO_2/km found in the present study is higher than the range of 140-150 g CO_2/km reported by Zurita et al. [32], who used standardized driving cycles (for example, New European Driving Cycle (NEDC) and Federal Test Procedure (FTP) 75) to evaluate the performance of a Chevrolet Aveo under controlled laboratory conditions. This demonstrates the importance of a vehicle being evaluated with driving cycles that reflect the actual kinematic conditions of the spatial domain in which the vehicle operates [33]. Otherwise, there may be a discrepancy between the values obtained in type-approval processes and those obtained in real traffic conditions. Overall, these results demonstrate that the vehicle and its engine performed better in highway conditions. Hence, to improve engine performance, especially in urban conditions, the use of start-stop technologies in engines is a valid strategy [28]. This leads to reduced engine running times in low load ranges (idle conditions), which are characterized by low fuel efficiency as this study has shown.

TABLE IV
OVERALL ENGINE PERFORMANCE OF FUEL EFFICIENCY, ENERGY EMISSIONS, EMISSION RATES, AND DISTANCE EMISSIONS (FROM VEHICLE) BY ROAD SECTION

Road section	Average value (%)	Energy-emission factors (g/kWh)		Average emission rates (g/s)		Distance-emission factors (g/km)	
	BTE	BSFC	CO_2	FC	CO_2	FC	CO_2
Urban	0.25	287.01	765.28	0.39	1.23	78.21	241.50
Suburban	0.27	244.81	654.74	0.76	2.35	51.49	159.01
Motorway	0.31	250.18	692.06	1.34	4.14	52.11	160.91
All sections	0.27	275.26	716.72	0.59	1.84	61.58	190.14

V. Conclusion

Under real traffic conditions a vehicle interacts with the road, other vehicles, and traffic control devices. The level of traffic influences driving patterns and, consequently, this could affect travel times, fuel consumption and emission levels of vehicles. In this context, this study aimed to create contour engine maps of fuel consumption and CO_2 emissions from a vehicle operating under real-world traffic conditions. A typical gasoline-powered light vehicle from the ecuadorian car fleet was chosen for the experimental campaign developed on an RDE route. This study presents a novel methodology for constructing two-dimensional engine contour maps using real-time recording of engine and vehicle parameters from the OBD system.

The results showed that the engine of the tested vehicle operated with a BTE of 27 %, a BSFC of 275 g/kWh, and a CO_2 energy-emission factor of 716 g/kWh under real traffic conditions. Furthermore, in terms of distance, the CO_2 emission factor for the tested vehicle was approximately 190 g/km. Overall, these results demonstrate two aspects: (I) the tested vehicle and its engine had lower fuel efficiency for urban conditions, which were characterized by frequent engine operation at low-load conditions; and (II) it was demonstrated that the OBD approach is a valid method to evaluate the performance of a vehicle in real traffic conditions. Hence, the OBD approach is a valid alternative for Latin American countries, where PEMS equipment is not readily available. Finally, it is important to note that the resulting engine maps of this study include valuable information that can be used as input data for vehicle simulators, as well as for developing emission inventories in cities.

ACKNOWLEDGEMENT

The authors would like to thank Andrés Espinosa and Luis Cuzco, those who contributed to the experimental campaign carried out as part of this study.

REFERENCES

[1] H. C. Frey. “Trends in Onroad Transportation Energy and Emissions,” *Journal of the Air & Waste Management Association.*, vol. 68, no. 6, pp. 514-563, 2018, doi: 10.1080/10962247.2018.1454357.

[2] Instituto de Investigación Geológico y Energético del Ecuador, “Balance Energético Nacional del Ecuador 2021,” Quito, Ecuador, 2022. [Online]. Available: https://www.recursosyenergia.gob.ec/wp-content/uploads/2022/08/Balance_Energético_Nacional_2021-VF_opt.pdf.

[3] F. Rosero, N. Fonseca, J.M. López, and J. Casanova. “Effects of Passenger Load, Road Grade, and Congestion Level on Real-World Fuel Consumption and Emissions from Compressed Natural Gas and Diesel Urban Buses,” *Applied Energy*, vol. 282, no. November 2020, p. 116195, Jan. 2021, doi: 10.1016/j.apenergy.2020.116195.

[4] EPA, NHTSA, and DOT. *Greenhouse Gas Emissions and Fuel Efficiency Standards for Medium- Heavy-Duty Engines and Vehicles-Phase 2*, vol. 81, no. 206. 2016, pp. 73478-74274.

[5] EU. “Commission Regulation (EU) No 582/2011 Of 25 May 2011 Implementing and Amending Regulation (EC) No 595/2009 of the European Parliament and of the Council With Respect to Emissions From Heavy Duty Vehicles (Euro VI) and Amending Annexes I And III to Direct,” *Official Journal of the European Union*, 2011. https://eur-lex.europa.eu/eli/reg/2011/582/oj.

[6] F. Posada and A. Bandivadekar. “Global Overview of On-Board Diagnostic (OBD) Systems for Heavy-Duty Vehicles,” *ICCT*, no. January, 2015.

[7] Á. Ramos, R. García-Contreras, and O. Armas. “Performance, Combustion Timing and Emissions from a Light Duty Vehicle at Different Altitudes Fueled with Animal Fat Biodiesel, GTL and Diesel Fuels,” vol. 182, pp. 507-517, 2016, doi: 10.1016/j.apenergy.2016.08.159.

[8] European Commission and Council of the European Union. “Commission Regulation (EU) 2016/427 Amending Regulation (EC) No 692/2008 as Regards Emissions from Light Passenger and Commercial Vehicles (Euro 6) (Text With EEA Relevance),” *Official Journal of the European Union*, vol. 82, no. 31/03/2016, pp. 1-98, 2016, [Online]. Available: http://data.europa.eu/eli/reg/2016/427/oj.

[9] J. M. Luján, V. Bermúdez, V. Dolz, and J. Monsalve-Serrano. “An Assessment of the Real-World Driving Gaseous Emissions from a Euro 6 Light-Duty Diesel Vehicle Using a Portable Emissions Measurement System (PEMS),” *Atmospheric Environment,* vol. 174, no. July 2017, pp. 112-121, 2018, doi: 10.1016/j.atmosenv.2017.11.056.

[10] European Commission. “Commission Regulation (EU) 2017/1151 of 1 June 2017 Supplementing Regulation (EC) No 715/2007 of the European Parliament and of the Council on Type-Approval of Motor Vehicles with Respect to Emissions from Light Passenger and Commercial Vehicles (Euro 5 a)” *Official Journal of the European Union,* no. 692, pp. 1–643, 2017.

[11] Y. Wen, et al. “A Data-Driven Method of Traffic Emissions Mapping with Land use Random Forest Models,” *Applied Energy*, vol. 305, no. July 2021, 2022, doi: 10.1016/j.apenergy.2021.117916.

[12] W. He, L. Duan, Z. Zhang, X. Zhao, and Y. Cheng. “Analysis of the Characteristics of Real-World Emission Factors and VSP Distributions. A Case Study in Beijing,” *Sustainability*, vol. 14, no. 18, p. 11512, Sep. 2022, doi: 10.3390/su141811512.

[13] J. D. K. Bishop, N. Molden, and A. M. Boies. “Using Portable Emissions Measurement Systems (PEMS) to Derive More Accurate Estimates of Fuel Use and Nitrogen Oxides Emissions from Modern Euro 6 Passenger Cars Under Real-World Driving Conditions,” *Applied Energy*, vol. 242, no. February, pp. 942-973, 2019, doi: 10.1016/j.apenergy.2019.03.047.

[14] Z. Mera, R. Varella, P. Baptista, G. Duarte, and F. Rosero.“Including Engine Data for Energy and Pollutants Assessment into the Vehicle Specific Power Methodology,” *Applied Energy*, vol. 311, no. February, p. 118690, Apr. 2022, doi: 10.1016/j.apenergy.2022.118690.

[15] J. Castresana, G. Gabiña, L. Martin, A. Basterretxea, and Z. Uriondo. “Marine Diesel Engine ANN Modelling with Multiple Output for Complete Engine Performance Map,” *Fuel*, vol. 319, no. March, 2022, doi: 10.1016/j.fuel.2022.123873.

[16] Z. Gao, J. C. Conklin, C. S. Daw, and V. K. Chakravarthy. “A Proposed Methodology for Estimating Transient Engine-Out Temperature and Emissions from Steady-State Maps,” *International Journal of Engine Research*, vol. 11, no. 2, pp. 137-151, 2010, doi: 10.1243/14680874JER05609.

[17] AEADE. “Anuario 2020 AEADE,” Quito, 2020. [Online]. Available: https://abimapi.com.br/anuario/pdf/anuario_2020-3.pdf.

[18] Instituto Nacional de Estadística y Censos (INEC). “Ecuador-Estadísticas de Transportes 2020,” Quito, 2021. [Online]. Available: https://anda.inec.gob.ec/anda/index.php/catalog/894/related_materials.

[19] RStudio. “RStudio: Integrated Development Environment for R.” Boston, MA, 2018.

[20] J. Wang, H. Rakha, L. C. Marr, P. Murray-Tuite, and I. El-Shawarby. “Multi-Modal Energy Consumption Modeling and Eco-routing System Development,” 2017, [Online]. Available: https://vtechworks.lib.vt.edu/bitstream/handle/10919/78624/Wang_J_D_2017.pdf?sequence=1&isAllowed=y.

[21] F. Rosero, N. Fonseca, J.-M. López, and J. Casanova. “Real-World Fuel Efficiency and Emissions from an Urban Diesel Bus Engine Under Transient Operating Conditions,” *Applied. Energy*, vol. 261, no. December 2019, p. 114442, Mar. 2020, doi: 10.1016/j.apenergy.2019.114442.

[22] H. Wickham. *Ggplot2: Elegant Graphics for Data Analysis*. Springer-Verlag New York, 2016.

[23] A. Quimbita and E. Guallichico. “Determinación del potencial energético y mecánico del motor Mazda F2 al utilizar los tipos de gasolina comercial empleados en el Ecuador,” Universidad de las Fuerzas Armadas - ESPE, 2017.

[24] J. B. Heywood. *Internal Combustion Engine Fundamentals*. New York: McGraw-Hill, 1988.

[25] J. D. K. Bishop, M. E. J. Stettler, N. Molden, and A. M. Boies. “Engine Maps of Fuel Use and Emissions From Transient Driving Cycles,” *Applied Energy*, vol. 183, pp. 202-217, 2016, doi: 10.1016/j.apenergy.2016.08.175.

[26] S. Tsiakmakis, et al. “From Lab-to-Road & Vice-Versa : Using a Simulation-Based Approach for Predicting Real-World CO_2 Emissions” *Energy*, vol. 169, pp. 1153–1165, 2019, doi: 10.1016/j.energy.2018.12.063.

[27] J. Gao, et al. “Fuel Consumption and Exhaust Emissions of Diesel Vehicles in Worldwide Harmonized Light Vehicles Test Cycles and Their Sensitivities to Eco-Driving Factors,” *Energy Conversion and Management*, vol. 196, no. May, pp. 605–613, 2019, doi: 10.1016/j.enconman.2019.06.038.

[28] G. Triantafyllopoulos, A. Dimaratos, L. Ntziachristos, Y. Bernard, J. Dornoff, and Z. Samaras. “A Study on the CO_2 and NO X Emissions Performance of Euro 6 Diesel Vehicles Under Various Chassis Dynamometer and On-Road Conditions Including Latest Regulatory Provi-

sions," *Science of the Total Environmen.*, vol. 66, no. x, pp. 337–346, 2019, doi: 10.1016/j.scitotenv.2019.02.144.

[29] E. G. Giakoumis and A. I. Alafouzos. "Study of Diesel Engine Performance and Emissions During a Transient Cycle Applying an Engine Mapping-Based Methodology," *Appied. Energy*, vol. 87, no. 4, pp. 1358–1365, 2010, doi: 10.1016/j.apenergy.2009.09.003.

[30] H. Steven and H. Steven. "VECTO Tool Development : Completion of Methodology to Simulate Heavy Duty Vehicles Fuel Consumption and CO_2 Emissions Upgrades to the Existing Version of VECTO and Completion of Certification Methodology to be Incorporated into a Commission legislative," no. I, 2017.

[31] F. Rosero, L. Garzón, and C. León. "Los patrones de viaje en taxi como herramienta de gestión de la movilidad urba," in *Tecnologías aplicadas a la Ingeniería*, Ibarra: Editorial UTN, 2017.

[32] B. J. Zurita and E. Llanes. "Comparativa de los factores de emisión entre el ciclo europeo y el FTP75 para un vehículo de ciclo otto categoría M1," Universidad Internacional SEK, 2022.

[33] J. Pavlovic, B. Ciuffo, G. Fontaras, V. Valverde, and A. Marotta. "How Much Difference in Type-Approval CO_2 Emissions from Passenger Cars in Europe Can be Expected from Changing to the New Test Procedure (NEDC Vs. WLTP)?," *Transportation Research,* vol. 111, no. October 2017, pp. 136–147, 2018, doi: 10.1016/j.tra.2018.02.002.